DEUTSCHES ELEKTRONEN-SYNCHROTRON DESY

DESY 76/34
July 1976

e^+e^--Annihilation into Baryon-Antibaryon Pairs

by

J. G. Körner and M. Kuroda

Abstract

Using GVDM-type form factors we calculate the e^+-e^- production cross sections for the reactions $e^+e^- \to \frac{1}{2}^+ - \frac{1}{2}^-$, $\frac{1}{2}^+ - \frac{1}{2}^-$, $\frac{3}{2}^+ - \frac{1}{2}^+$, $\frac{3}{2}^+ - \frac{3}{2}^+$ and $\frac{3}{2}^+ - \frac{3}{2}^+$ including all prominent baryon resonances at energies of present and planned e^+-e^- storage ring machines. We also evaluate the cross section of charmed baryon pair production. Near their respective thresholds charmed and uncharmed baryon pair production are predicted to constitute comparable fractions of the total hadronic cross section. The calculated cross sections indicate that the interference of direct and 1-photon decay of the ψ-particles into baryon pairs is small.

2 HAMBURG 52 · NOTKESTIEG 1

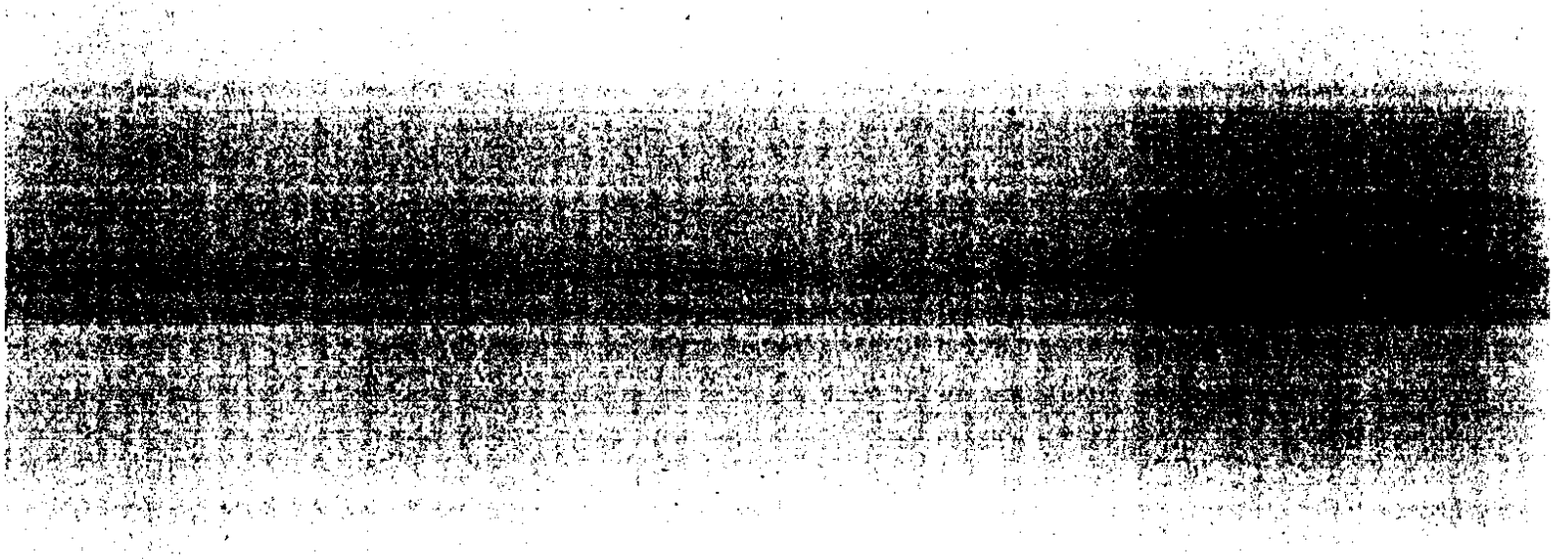

To be sure that your preprints are promptly included in the
HIGH ENERGY PHYSICS INDEX ,
send them to the following address (if possible by air mail) :

DESY
Bibliothek
2 Hamburg 52
Notkestieg 1
Germany

e^+e^--Annihilation into Baryon-Antibaryon Pairs

by

J. G. Körner and M. Kuroda[+]
Deutsches Elektronen-Synchrotron DESY, Hamburg

Abstract:

Using GVDM-type form factors we calculate the e^+-e^- production cross sections for the reactions $e^+e^- \to \frac{1}{2}^+ - \frac{1}{2}^\pm$, $\frac{1}{2}^+ - \frac{3}{2}^\pm$, $\frac{1}{2}^+ - \frac{5}{2}^+$ and $\frac{3}{2}^+ - \frac{3}{2}^+$ including all prominent baryon resonances at energies of present and planned e^+-e^- storage ring machines. We also evaluate the cross section of charmed baryon pair production. Near their respective thresholds charmed and uncharmed baryon pair production are predicted to constitute comparable fractions of the total hadronic cross section. The calculated cross sections indicate that the interference of direct and 1-photon decay of the ψ-particles into baryon pairs is small.

[+]Alexander von Humboldt Foundation Fellow

1. Introduction

In the next few years one anticipates in addition to total and inclusive e^+-e^- cross section measurements also data on exclusive two-body and quasi-two-body production cross sections which are expected to provide important information on the electro-magnetic structure of hadrons in the time-like region. Obviously the rate for the production of baryon-antibaryon pairs will be much suppressed compared to the production rate of meson pairs and will constitute only a minute fraction of the total production cross section at any given energy. The question then arises whether present and/or future machine luminosities and detection efficiencies are sufficient to collect enough data on baryon pair production to enable one to study this potentially rich area of physics. In order to answer this question we present some cross section estimates of two-body and quasi-two-body baryon pair production based on present knowledge of the form factor behaviour of elastic and inelastic baryon production in the space-like region (for previous estimates see [1,2]).

A principal problem in the calculation of annihilation cross sections into two-body and quasi-two-body states involving particles with spins is the appearance of kinematic q^2-powers which have to be damped by some dynamical mechanism in order not to violate general theoretical principles as e.g. unitarity bounds. In addition, if form factors have a dynamical power behaviour in q^2, one expects a relation between this power and the spins of the produced particles [3,4,5,6] for the Drell-Yan threshold relation to hold.

In the dual current model [5] this interrelation is realized through GVDM-type form factors which consist of a product of poles in the time-like region with pole positions located at the vector meson poles and their Veneziano recurrences. The product terminates at the appropriate recurrence to assure the validity of the Drell-Yan threshold relation [see e.g. [7]]. Such form factors were shown in Ref.[8] to give a good fit to the space-like transition form factor analysis of Devenish and Lyth [9] (for a comparison with elastic form factor data see Ref.[10]).

In this paper we extend the analysis of Ref.[8] to the time-like region. We calculate the production cross sections for all members of the ground state octet and decuplet with $J^P = \frac{1}{2}^+$ and $\frac{3}{2}^+$ in the processes $e^+e^- \to \frac{1}{2}^+\,\frac{1}{2}^+$, $\frac{3}{2}^+\,\frac{3}{2}^+$, $\frac{1}{2}^+\,\frac{3}{2}^+$ and resonance production in $e^+e^- \to N\,\overline{N^*}$, where we consider the

resonances $N^* = D_{13}(1520)$, $F_{15}(1688)$, $P_{11}(1470)$ and $S_{11}(1535)$ with $J^P = \frac{3}{2}^-, \frac{5}{2}^+, \frac{1}{2}^+$ and $\frac{1}{2}^-$ resp.. We also evaluate the production cross sections of some of the conjectured charmed baryons.

In particular in the latter case one observes the importance of using form factors with dynamical particle singularities instead of using some ad hoc parametrization as e.g. in the dipole form factor. In this way a new scale appropriate to the production of heavy particles enters into the form factors through the heavy vector mesons ψ, ψ'... . As will become apparent this implies that the peak cross sections of charmed and ordinary baryon production near their respective thresholds constitute comparable fractions of the total hadronic cross sections.

Our main results may be summarized as follows:

1) The cross sections rise steeply from threshold to their peak value and then decrease faster than what corresponds to a naive $(q^2)^{-5}$ power law in an intermediate q^2-region. The faster-than-$(q^2)^{-5}$ decrease is due to the presence of the vector meson mass singularities in the time-like region, and, for the "elastic" production reactions, due to destructive interference effects between the various contributing form factors. The cross sections are in general very small. For example, the peak cross section for $\Omega^-\bar{\Omega}^-$ production is predicted to be a mere 6×10^{-6} nb.

2) If the charmed baryon masses lie in the range $m_c = 2.5 \sim 3.0$ GeV, the ratio $\sigma_{c\bar{c}}/\sigma_{total}$ close to $q^2_{c\bar{c}\text{-threshold}}$ is comparable to $\sigma_{p\bar{p}}/\sigma_{total}$ close to $q^2_{p\bar{p}\text{-threshold}}$.

3) The 1-photon decay mode of the ψ-particle into baryon pairs is small and the interference with the direct decay is likely to occur only at a level of a few percent.

2. Form Factors

We shall be working with the constraint free form factors that have been introduced in Ref.[8]. It is then straightforward to obtain the relations between these and the c.m. helicity amplitudes which are given in the Appendix. Since the constraint free form factors are independent of each other for all values of q^2 the corresponding helicity amplitudes exhibit the correct

kinematical threshold and pseudothreshold constraint structure (see Ref.[8,11]).

As in Ref.[8] the q^2-dependence of the constraint free form factors is assumed to arise from the coupling of many vector mesons in the form of a product of poles. Thus we have for a form factor

$$F(q^2) = \sum_{i=\rho,\omega,\phi,\psi} C_i \prod_{n=0}^{N(J,c)-1} \left(1 - \frac{q^2}{m_i^2 + n\alpha_i'^{-1}}\right)^{-1} . \qquad (1)$$

The product in Eq.(1) extends over as many poles $N(J,c)$ as is necessary to satisfay the Drell-Yan threshold relation. Thus, for a given resonance, the resonance contributions to e.g. νW_2 should give $\nu W_2 \sim (\omega - 1)^{2c-1}$ in the limit $q^2 \to -\infty$, where c determines the threshold power in νW_2 and is set to $c = 2$ for canonical dipole behaviour. Also we shall assume asymptotic suppression of longitudinal resonance contributions. In the time like region these assumptions lead to $\sigma_T \sim (1/q^2)^{2c+1}$ and $\sigma_L/\sigma_T \sim (1/q^2)$ for the annihilation cross sections defined in Appendix A.

The sum in Eq.(1) extends over the different vector mesons ρ,ω,ϕ and ψ and their recurrences that couple to the photon. In terms of the quark language we decompose the photon according to the contributions $(2)^{-1/2}(u\bar{u} + d\bar{d})$, $(2)^{-1/2}(u\bar{u} - d\bar{d})$, $(\lambda\bar{\lambda})$ and $(c\bar{c})$. We shall ignore the small deviations from ideal mixing for ω, ϕ and ψ and assume the complete validity of the OZI rule [12]+. The resulting couplings are given in the Appendix B.

For the Regge slopes α_i' appearing in Eq.(1) we shall use $\alpha' \simeq 0.9 - 1.0$ GeV^{-2} for the uncharmed vector mesons and $\alpha' = 0.25$ GeV^{-2} for the sequence ψ, ψ',... treating the ψ' as the first Veneziano recurrences of ψ. For the masses of the lowest lying vector mesons we use $m_\rho^2 = 0.593$ GeV^2, $m_\omega^2 = 0.614$ GeV^2, $m_\phi^2 = 1.040$ GeV^2 and $m_\psi^2 = 9.579$ GeV^2.

The motivation for using such product type GVDM form factors is provided by the dual current model [5] which predicts such a form factor behaviour for leading resonance excitation [7]. As has been shown in Ref.[8], such form factors can

+Inclusion of effects due to small deviations from ideal mixing would affect our results only insignificantly.

account quite well for the space-like q^2-behaviour of some of the resonance excitation data.

In general the $q^2 = 0$ values of the form factors will be determined from data if possible. In some cases some additional theoretical input has to be used which will be discussed in Sec.3.

Finally we remark that we shall always be working in the narrow resonance approximation for the vector mesons. This is well justified since the production thresholds of all the cases treated here are at least 1 GeV^2 above the highest lying vector meson pole coupling to the respective production amplitude.

3. Cross Sections

The kinematic quantities used in this section are all defined in Appendix A. We shall not in every case be referring to the relevant equations in the Appendix.

a) $\frac{1^+}{2} - \frac{\overline{1^+}}{2}$ Production

The canonical dipole behaviour corresponds to the choice of Λ^2 poles for $F_1(q^2)$ and 3 or more poles for $F_2(q^2)$. We shall represent $F_2(q^2)$ by 3 poles, i.e. the minimum number of poles required to satisfy the Drell-Yan relation. The F_1 are normalized to the charge at $q^2 = 0$ and the $F_2(0)$ to the anomalous magnetic moment. For p, n, Λ, Σ^+ and Ξ^- we use the experimental magnetic moments as input and for the remaining members of the octet including the $\Sigma^0\overline{\Lambda}$ transition moment SU(6) values. The tabulated values of relative ρ, ω and ϕ couplings in Appendix B correspond to pure F-coupling for $F_1(0)$ and the SU(6) F/D-ratio F/D = 2/3 for $G_M(0)$.

In Figs.1 and 2 we compare our form factors with the experimental proton and neutron form factors from the analysis of Felst [13]. In the case of the magnetic form factor of the proton G_M^p better agreement with the data is obtained for $\alpha' = 1$, whereas there is not much difference between $\alpha' = 0.9$ and $\alpha' = 1$ for the other three cases G_E^p, G_M^n and G_E^n. The gross features of the form factor behaviour are reproduced quite well and the deviations from the experimental values are within approximately 10%.

In Fig.3 we show our predictions for the production cross sections. For $p\bar{p}$ production the calculated cross section close to threshold is quite sensitive to the choice $\alpha' = 0.9$ or $\alpha' = 1.0$ due to destructive interferences between the two pole ansatz of F_1 and the three pole ansatz of F_2. For $\alpha' = 0.9$ and $\alpha' = 1.0$ our predicted cross sections are within 1 and 3 standard deviations resp. of the Frascati measurement at $q^2 = 4.41$ GeV^2 [14]$^+$. For higher values of q^2 the predicted $p\bar{p}$ cross sections for the two different values of α' approach one another and lie within ~ 15% for $q^2 = \infty$. Whereas the spacelike data seems to favour a slope of $\alpha' = 1$ the value $\alpha' = 0.9$ is more favourable for a fit through the Frascati point. In the case of $n\bar{n}$ production the interference between F_1 and F_2 is negligible ($F_1^n(q^2) \equiv 0$ for $m_\omega^2 = m_\rho^2$) resulting in a larger cross section in the intermediate q^2-region. For the same reason the difference between choosing $\alpha' = 1.0$ or $\alpha' = 0.9$ is small in this case. Since it is at present rather difficult to commit oneself to a definite value for the spacing of the vector mesons and their recurrences one has to accept our results modulo this uncertainty in the slope value. At any rate, except for a region close to threshold our results are not so extremely sensitive to the value of the Regge slope. The remaining figures are drawn for $\alpha' = 1$.

In Ref.[15] a detailed analysis of elastic proton and neutron form factor data was performed using a parametrization in terms of vector mesons. Apart from the usual $q^2 = 0$ constraints most of the masses and residues of the vector meson recurrences were treated as free parameters. In our treatment the only free parameter is the Regge slope α' which is constrained to vary in a limited range only. It is clear that we can therefore only expect to reproduce the gross features of the form factor behaviour in the space-like region. Expanding our product-type form factors in terms of sums of vector meson contributions one obtains residues which show the alternating sign pattern characteristic of all form factor fits. However, the values of the residues are in general different from those in Ref.[15]. Our residues reflect the asymptotic constraints which we imposed from the outset, whereas in the treatment of Ref.[15] no such constraints are used.

It is well known that different satisfactory fits to the elastic space-like

---

$^+$ A slight downward readjustment (~4%) of the Frascati total cross section value would result if our $|G_M| \neq |G_E|$ were taken instead of the assumption of angular isotropy as in Ref.[14].

data can lead to widely varying predictions in the time-like region. For example, Renard maintains that finite width effects and inelasticity corrections to the vector meson propagators are important and he arrives at a satisfactory representation of the space-like data [2]. He presents $p\bar{p}$-production cross sections that are rather large. Independent of the details of his model the large cross sections can be traced to an ad hoc assumption about how F_1 and F_2 are related to one another. This assumption produces a strong constructive interference in the time-like region between the contributions of the two form factors which leads to a big cross section.

In Fig.(3a) we have also included upper bounds from Ref.[16,17]. A preliminary upper bound of 6×10^{-2} nb at $q^2 = 9$ GeV^2 due to a tentative $p\bar{p}$ event is reported from Spear [18].

The cross sections for the other reactions such as $e^+e^- \to \Sigma^+\bar{\Sigma}^+$, $\Lambda\bar{\Lambda}$ etc. are small and are therefore expected to be measurable only near the threshold where the cross sections peak at $10^{-2} - 10^{-1}$ nb. The cross section for $\Xi^-\bar{\Xi}^-$ production shows a broad shoulder around $\sqrt{q^2} \sim 3$-4 GeV which again is due to interference effects between F_1 and F_2.

We close this subsection by remarking that the asymptotic constraints we impose on the q^2-behaviour of F_1 and F_2 are also compatible with F_2 having 4 poles. The fit to the space-like data would not be affected so much by such a choice. However, in the time-like region F_1 and F_2 would now constructively interfer. We have checked that such a choice would not be compatible with the Frascati point and the upper bounds provided by [16,17]. For example, at the Frascati point the $p\bar{p}$ cross section would be more than 20 times the experimental value.

b) $\frac{3^+}{2}\,\frac{\overline{3^+}}{2}$ Production

The canonical choice for F_1, F_2, F_3 and F_4 is 3,4,4 and 5 poles. From SU(6) [19] or from the quark model including effects due to the difference of current and constituent quarks [20] one has for the multipoles

$$
\begin{aligned}
G_E(0) &= F_1(0) = Q \quad , \\
G_M(0) &= F_1(0) + F_2(0) = Q\mu_p \quad , \\
G_Q(0) &= F_1(0) - F_3(0) = 0 \quad , \\
\sqrt{6}\, G_\sigma(0) &= F_1(0) + F_2(0) - F_3(0) - F_4(0) = 0 \quad ,
\end{aligned}
\tag{2}
$$

where Q is the charge and μ_p is the magnetic moment of the proton. We show the results for $e^+e^- \to \frac{3^+}{2}\,\frac{\overline{3^+}}{2}$ in Fig.4. The Δ^{++}-pair production has the largest cross section in the decuplet which is due to its double charge and its lightness. Although the $\Omega^-\bar{\Omega}^-$ production cross section is enhanced by the ϕ-meson dominance of its form factos its cross section is small ($\sim 10^{-5}$ nb at peak value) and thus the direct electromagnetic production of Ω^--pairs will be extremely hard to observe. After reaching its peak value the $\Omega^-\bar{\Omega}^-$ production decreases at a slower rate than the $\Delta\bar{\Delta}$ cross section, since $\Omega^-\bar{\Omega}^-$ production occurs at higher q^2-values.

c) $\frac{1^+}{2}\,\frac{\overline{3^+}}{2}$ Production

The canonical choice for the three form factors G_1, G_2 and G_3 is 3, 3 and 4 poles. However, in Ref.[8] it was shown that the form factor data requires a one-below-canonical form factor behaviour, which is in nice accord with theoretical ideas related to the attainment of the value $\frac{1}{4}$ for the ratio $\nu W_2^n/\nu W_2^p$ in the threshold region $\omega \to 1$ [21]. A good fit to the space-like data [9,22] was obtained for $\gamma_v p \to \Delta^+$ using

$$
\begin{aligned}
G_1(0)/M &= 1.77 \text{ GeV}^{-2} \quad , \\
G_2(0) &= -1.31 \text{ GeV}^{-2} \quad , \\
G_3(0) &= 0 \quad ,
\end{aligned}
\tag{3}
$$

and using 4 poles for G_1 and G_2 (Fig.5)(see also [8]). A choice of $G_1(0)/M\, G_2(0) = -1$ in Eq.(3) would correspond to a pure M1 transition as predicted by SU(6)(see e.g.[19]) or the quark model (see e.g. Ref.[20]). However, the deviation from this value indicated in Eq.(3) allows for the small E2 and Coulombic contributions that are observed in the data (see Fig.5).

Our results are shown in Fig.6. Since G_1 and G_2 have dimensions of -1 and -2,

we have multiplied these by M and M^2 in order to apply SU(3) to dimensionless couplings. The resulting predictions for the various cross sections are of course subject to the well-known ambiguities connected with the choice of mass factors that are used to obtain the dimensionless couplings.

d) $\frac{1}{2}^+ - \overline{\frac{3}{2}^-}$ Production $[D_{13}(1520)]$

In Ref.[8] a reasonable fit to the results of the analysis of Devenish and Lyth [9] was found for the canonical choice G_1' and G_2' with three poles each. For the mass we take $M = 1.514$ GeV [9].

The coupling values at $q^2 = 0$ are

$$\begin{aligned} G_1'^+(0)/M &= 1.73\ \text{GeV}^{-2} & G_1'^0(0)/M &= -0.008\ \text{GeV}^{-2} \\ G_2'^+(0) &= 1.38\ \text{GeV}^{-2} & G_2'^0(0) &= 0.671\ \text{GeV}^{-2} \\ G_3'^+(0) &= 0 & G_3'^0(0) &= 0 \end{aligned} \tag{4}$$

for the charge (+) and (0) members of the isodoublet. The resulting prediction is shown in Fig.7.

e) $\frac{1}{2}^+ - \overline{\frac{5}{2}^+}$ Production $[F_{15}(1688)]$

One has ($M = 1.682$ [9])

$$\begin{aligned} G_1'^+(0)/M &= 2.10\ \text{GeV}^{-3} \\ G_2'^+(0) &= 1.14\ \text{GeV}^{-3} \\ G_3'^+(0) &= 0 \end{aligned} \tag{5}$$

and the canonical choice of 4 poles. The coupling of the neutral isobar state is small (see e.g. [23]). Results are shown in Fig.7.

f) $\frac{1}{2}^+ - \overline{\frac{1}{2}^+}$ $[P_{11}(1470)]$ and $\frac{1}{2}^+ - \overline{\frac{1}{2}^-}$ $[S_{11}(1535)]$ Production

At present a reliable prediction of the production cross sections of these two baryon resonances is rather difficult for the following reasons. Experimentally the q^2-dependence of the respective multipoles in the space-like region are not determined in a very reliable way. The multipoles of these two resonances as determined from the fit procedure of Ref.[9] are quite sensitive to input assumptions and tend to be unstable [24]. Theoretically their form factors cannot be expected to have as simple a form as the transition form factors of the leading baryon resonances since S_{11} and P_{11} occur at daughter level. One would have to reach a better understanding of the q^2-dependence of these multipoles in the space-like region before one could continue to the time-like region with much confidence.

Nevertheless we take the results of Ref.[8] and attempt a continuation to the time-like region by using an effective form factor parametrization of the space-like data. For the $S_{11}^+(1535)$ such an <u>effective</u> parametrization is given by

$$\begin{aligned} G_1'^+(0) &= -1.31\ \text{GeV}^{-2} \\ G_2'^+(0) &= 0.25\ \text{GeV}^{-2} \end{aligned} \tag{6}$$

$m^2_{V\ \text{eff.}} = 0.35\ \text{GeV}^2$, $\alpha'_{\text{eff.}} = 1.3\ \text{GeV}^{-2}$ with (the canonical) 3 poles each for $G_1'(q^2)$ and $G_2'(q^2)$. We use $M = 1.505$ GeV [9]. Similarly for the $P_{11}^+(1470)$ (We use $M = 1.434$ GeV [9])

$$\begin{aligned} G_1^+(0) &= 1.57\ \text{GeV}^{-2} \\ G_2^+(0) &= 1.33\ \text{GeV}^{-2} \end{aligned} \tag{7}$$

$m^2_{V\ \text{eff.}} = 0.08\ \text{GeV}^2$, $\alpha'_{\text{eff.}} = 1.5\ \text{GeV}^{-2}$ and (the canonical) 3 poles each for $G_1(q^2)$ and $G_2(q^2)$. We stress that the vector mesons appearing in the parametrization of the form factors are meant to represent only <u>effective</u> pole parametrizations and we do not mean to imply that such particle singularities exist.

Our predictions are shown in Fig.7. As emphasized before, these predictions must at present be considered tentative at best.

g) Estimate of Three-Body Production Rates

The three-body production processes $e^+e^- \to p\bar{p}\pi^0$ and $e^+e^- \to p\bar{p}\,\eta$ are estimated by assuming that the two-body subsystems $p\pi^0$, $\bar{p}\pi^0$ etc. result from the decay of one of the resonance states P_{11}, S_{11}, P_{33}, D_{33} and F_{15}. Using the known branching ratios of these resonances into $p\pi^0$ and $p\eta$ we show our estimates for the production of $p\bar{p}\,\pi^0$ and $p\bar{p}\,\eta$ in Fig.8. We do not give any figures for the other three-body charge states because we lack complete information on the neutral quasi-two-body states. It is difficult to estimate the contribution from non-resonant background and from coherence effects. Fig.8 should therefore be interpreted as giving a lower bound on $p\bar{p}\pi^0$ and $p\bar{p}\eta$ production (see also [1]).

Compared to the rate estimates of Ref.[1] our $p\bar{p}\pi^0$ cross section is down by approximately 3 orders of magnitude. The large production cross sections of Ref.[1] may have resulted from using too large time-like form factors.

We would like to mention that a preliminary upper bound for $p\bar{p}\pi^0$ production at $q^2 = 9\ \mathrm{GeV}^2$ is reported from Spear at 0.1 nb [18].

4. Comments

With the availability of high c.m. energies in colliding beam machines pair production of the conjectured charmed baryons may become a real possibility in the near future. We shall consider the pair production of the presumably lightest charmed baryons in the $J = \frac{1}{2}$ SU(4) ground state 20'-plet, the I = 0 state C_0^+ with quark content (cud), and the isotriplet C_1^{++}, C_1^+ and C_1^0 with quark content (cuu), (cud) and (cdd). The relative contributions of ρ, ω, ϕ and ψ are again fixed by the OZI rule and are given in Appendix B. The magnetic moments are calculated according to SU(4).+ For the masses we take the estimates of Gaillard, Lee and Rosner [25], i.e. $m_{C_0} \approx 2.6$ GeV and $m_{C_1} \approx 2.7$ GeV. The resulting prediction is shown in Fig.9. A characteristic feature of charmed baryon production are the relatively large peak cross sections. This results directly from the dominance of the "heavy" vector mesons in the form factors and can be easily understood from the observation that the ψ-family of vector mesons introduces a new mass scale into the form factors.++ In the same way the heavy vector meson poles are responsible for strong SU(4)-breaking effects for the current-matrix elements away from $q^2 = 0$. We have also checked that the results are not very sensitive to the assumed masses of the charmed

+Inclusion of SU(4) breaking effects in the calculation of the magnetic moments of the charmed baryons could possibly result in smaller cross section predictions.

++The possibility of obtaining large charmed baryon-antibaryon production cross sections in e^+e^- annihilation through ψ-vector meson dominance has been remarked on by previous authors (see e.g. Ref.[25]).

baryons. In Fig.9 we have also plotted our cross section predictions for masses $m_{C_0} = 3.0$ GeV and $m_{C_1} = 3.1$ GeV. It is apparent that the cross sections are approximately the same for different masses at a given value of q^2. For the lower mass values the peak cross sections constitute 2-5% of the total hadronic cross sections, whereas for the higher mass values they make up less than 1% (C_0^+) and 1 % (C_1^{++}). On the other hand, one could not take the charmed baryon masses to be much lower than the assumed lower values $m_C = 2.6$-2.7 GeV, since the predicted charmed baryon pair production cross sections would then saturate and even exceed the total hadronic production rate. The fact that the production cross sections in Fig.9 decrease relatively slowly with energy is due to the fact that charmed baryon production occurs at relatively high q^2-values.

Recently several authors have discussed the possibility of using the interference of 1-photon decay and direct decay of the ψ particles into some given final state to study the SU(3) properties of the ψ-decays [27]. Using the results of Sec.3 we can estimate the strength of such interference effects.

Let us first consider the decay $\psi \to \Lambda\bar{\Sigma}^0$ which occurs only via the 1-photon intermediate state $\psi \to \gamma \to \Lambda\bar{\Sigma}^0$, since the ψ is an isosinglet. From factorization one has

$$\frac{\Gamma(\psi \to \Lambda\bar{\Sigma}^0)}{\Gamma(\psi \to \mu^+\mu^-)} = \frac{\sigma(e^+e^- \to \gamma \to \Lambda\bar{\Sigma}^0)}{\sigma(e^+e^- \to \gamma \to \mu^+\mu^-)}\Bigg|_{q^2 = m_\psi^2} = 8.8 \times 10^{-5} \qquad (8)$$

using the results of Sec.3. Experimentally $\Gamma(\psi \to \Lambda\bar{\Sigma}^0)/\Gamma(\psi \to p\bar{p}) < 0.1$ [28] $\Gamma(\psi \to p\bar{p})/\Gamma(\psi \to all) = 0.0023 \pm 0.0006$ [29] giving for the above ratio an upper bound of 3.3×10^{-3} which is consistent with our prediction.

In a similar way we can calculate the partial decay rates $\psi \to N\bar{\Delta}$ since these decays also proceed via the 1-photon intermediate state. Using the results of Sec.3 we obtain for $\Gamma(\psi \to N\bar{\Delta} \to p\bar{p}\pi^0 + p\bar{n}\pi^- + n\bar{p}\pi^+)/\Gamma(\psi \to all) = 3.8 \times 10^{-5}$.

Experimentally one has $\Gamma(\psi \to p\bar{p}\pi^0 + p\bar{n}\pi^- + n\bar{p}\pi^+)/\Gamma(\psi \to all) = (3.7 \pm 1.9) \times 10^{-3}$ [30]. This would imply that a Dalitz plot analysis of the decay $\psi \to N\bar{N}\pi$ would show a Δ-enhancement only at the 1% level.

In the case $\psi \to p\bar{p}$ both the direct and 1-photon decay contribute. One has

$$\frac{\Gamma(\psi\to p\bar{p})}{\Gamma(\psi\to\mu^+\mu^-)} = \frac{\sigma(e^+e^-\to\psi\to\gamma\to p\bar{p})}{\sigma(e^+e^-\to\psi\to\mu^+\mu^-)} + \frac{\sigma(e^+e^-\to\psi\to p\bar{p})}{\sigma(e^+e^-\to\psi\to\mu^+\mu^-)} \quad (9)$$

+ interference term.

The first term on the r.h.s. of Eq.(9) is evaluated from our $p\bar{p}$ production cross section to be 3.3×10^{-5} ($\alpha' = 0.9$), which is negligible compared to the experimental value 0.033 ± 0.010 of the l.h.s. [29]. Therefore the direct decay accounts for almost 100% of the $\psi \to p\bar{p}$ rate. Numerically one obtains $\approx 3 \times 10^{-2}$ for the ratio of the 1-photon and direct decay amplitudes. This value is so small that it will be rather difficult to establish such an interference effect.

We close by remarking that, if the conclusions of this paper are correct, the measurement of baryon-antibaryon pair production off the ψ-resonances may be difficult but not impossible.

ACKNOWLEDGEMENT:

We would like to thank L. Criegee, D. Cords, R. Felst, G. Kramer, M. Krammer, T. Suda, G. Wolf and S. Yamada for discussions and for providing us with experimental information.

APPENDIX A

In Ref.[11,31] it was shown that, in the one photon approximation, the differential cross section for the annihilation into two particles with mass, helicity and momentum M, λ^*, p^* and m, λ, p resp., is given by

$$\frac{d\sigma}{d\cos\theta} = \frac{d\sigma_T}{d\cos\theta} + \frac{d\sigma_L}{d\cos\theta} \quad , \quad (A1)$$

where

$$\frac{d\sigma_T}{d\cos\theta} = 2\pi \frac{\alpha^2 p_c}{4(q^2)^2\sqrt{q^2}} \frac{1}{2} \sum_\lambda \left(|\Gamma^{\lambda+1,\lambda}|^2 + |\Gamma^{\lambda-1,\lambda}|^2 \right)(1+\cos^2\theta)$$

$$\frac{d\sigma_L}{d\cos\theta} = 2\pi \frac{\alpha^2 p_c}{4(q^2)^2\sqrt{q^2}} \sum_\lambda |\Gamma^{\lambda,\lambda}|^2 \sin^2\theta \quad . \quad (A2)$$

The $\Gamma^{\lambda^*,\lambda}$ are the c.m. helicity amplitudes with helicites λ and λ^* and p_c is the magnitude of the c.m. momentum. The total cross sections σ_T and σ_L are obtained from (A2) by cos θ -integration.

1) $\frac{1}{2}^+ - \frac{1}{2}^+$; equal mass case M = m

One defines constraint free gauge invariant form factors by

$$\langle N(p^*,\lambda^*)\bar{N}(p,\lambda)|J_\mu(0)|0\rangle = e\,\bar{u}(p^*,\lambda^*)\left[F_1\gamma_\mu + F_2\frac{i\sigma_{\mu\nu}q^\nu}{2m}\right]v(p,\lambda), \quad (A3)$$

where $q = p^* + p$.

The helicity amplitudes are given by

$$\Gamma^{1/2,1/2} = -2m(F_1+\eta F_2) = -2mG_E \quad ,$$
$$\Gamma^{1/2,-1/2} = \sqrt{2q^2}(F_1+F_2) = \sqrt{2q^2}\,G_M \quad , \tag{A4}$$

where $\eta = q^2/4m^2$.

Here and in the following cases we shall be listing only the independent helicity amplitudes. The other helicity amplitudes entering in the cross section formula Eq.(A2) can be obtained from parity and charge conjugation invariance (see Ref.[11,31]).

The differential cross section is given by

$$\frac{d\sigma}{d\cos\theta} = \frac{4\pi\alpha^2 p_c m^2}{(q^2)^2\sqrt{q^2}}\left[\sin^2\theta\,|G_E|^2 + \eta(1+\cos^2\theta)|G_M|^2\right] . \tag{A5}$$

2) $\frac{1}{2}^+ - \overline{\frac{1}{2}^+}$; unequal mass case

One defines constraint free amplitudes by (see Ref.[8])

$$\langle N^*(p^*,\lambda^*)\bar{N}(p,\lambda)|J_\mu(0)|0\rangle = e\,\bar{u}(p^*,\lambda^*)\Gamma_\mu\, v(p,\lambda),$$
$$\Gamma_\mu = F_1'(q^2\gamma_\mu - \not{q}q_\mu) + F_2'(P\cdot q\,\gamma_\mu - P_\mu\not{q}) \quad , \tag{A6}$$

where $P = \frac{1}{2}(p^* - p)$.

The transverse and longitudinal helicity amplitudes are

$$\Gamma^{1/2,-1/2} = \sqrt{\tfrac{1}{2}}\sqrt{Q^-}\,(2q^2F_1' + \sigma F_2') \quad ,$$
$$\Gamma^{1/2,1/2} = -\tfrac{1}{2}\sqrt{Q^-}\sqrt{q^2}\,(2(M+m)F_1' + (M-m)F_2') \quad , \tag{A7}$$

where we have introduced the abbreviations $Q^\pm = q^2 - (M\pm m)^2$ and $\sigma = M^2-m^2$. We caution the reader that some care has to be exercised to take the equal mass limit $M = m$ of Eq.(A7).

3) $\frac{1}{2}^+ - \overline{\frac{1}{2}^-}$

One defines corresponding unprimed amplitudes by multiplying Γ_μ by $i\gamma_5$ from the left:

$$\Gamma_\mu = i\gamma_5 F_1(q^2\gamma_\mu - \not{q}q_\mu) + i\gamma_5 F_2(P\cdot q\,\gamma_\mu - P_\mu\not{q}) \quad . \tag{A8}$$

The corresponding helicity amplitudes are given by the replacement $F_i \to F_i'$ and $M \leftrightarrow -M$ in Eq.(A7).

4) $\frac{3}{2}^+ - \overline{\frac{3}{2}^+}$

Constraint free gauge invariant form factors are defined by

$$\langle N_{3/2^+}(p^*,\lambda^*)\bar{N}_{3/2^+}(p,\lambda)|J_\mu(0)|0\rangle = e\,\bar{u}^\alpha(p^*,\lambda^*)\Gamma_{\alpha\beta\mu}u^\beta(p,\lambda), \tag{A9}$$

with

$$\Gamma_{\alpha\beta\mu} = g_{\alpha\beta}\left(F_1\gamma_\mu + F_2\frac{i\sigma_{\mu\nu}q_\nu}{2M}\right) + \frac{q_\alpha q_\beta}{2M^2}\left(F_3\gamma_\mu + F_4\frac{i\sigma_{\mu\nu}q_\nu}{2M}\right) . \tag{A10}$$

The four independent helicity amplitudes are given by

$$\Gamma^{3/2,1/2} = \sqrt{\tfrac{2}{3}}\sqrt{q^2}\,(F_1+F_2) \quad ,$$
$$\Gamma^{1/2,-1/2} = \tfrac{2}{3}\sqrt{2}\sqrt{q^2}\left[-(1-2\eta)(F_1+F_2) - 2\eta(1-\eta)(F_3+F_4)\right] \quad , \tag{A11}$$
$$\Gamma^{3/2,3/2} = -2M\,(F_1+\eta F_2) \quad ,$$
$$\Gamma^{1/2,1/2} = (1-\tfrac{4}{3}\eta)2M(F_1+\eta F_2) + \tfrac{4}{3}\eta(1-\eta)2M(F_3+\eta F_4) .$$

It is often convenient to work with multipole amplitudes [32] which are given by

$$G_E = \frac{1}{4M\sqrt{1-\eta}}\left(-\Gamma^{3/2,3/2} + \Gamma^{1/2,1/2}\right) ,$$
$$G_M = \frac{3}{5\sqrt{2}}\frac{1}{\sqrt{1-\eta}}\frac{1}{\sqrt{q^2}}\left(\sqrt{3}\,\Gamma^{3/2,1/2} - \Gamma^{1/2,-1/2}\right) , \qquad (A12)$$
$$G_Q = -\frac{3}{2\eta\sqrt{1-\eta}}\frac{1}{4M}\left(\Gamma^{3/2,3/2} + \Gamma^{1/2,1/2}\right) ,$$
$$G_\Theta = \frac{1}{4\eta\sqrt{1-\eta}}\frac{1}{\sqrt{q^2}}\left(\Gamma^{3/2,1/2} + \frac{\sqrt{3}}{2}\Gamma^{1/2,-1/2}\right) ,$$

and which, at $q^2 = 0$, are normalized to the charge (in units of e), magnetic dipole moment (in units of e/2M), electric quardrupole moment (inunits of e/M^2) and magnetic octupole moment (in units of $e/2M^3$).

In terms of the multipole amplitudes one has for the differential cross section

$$\frac{d\sigma}{d\cos\Theta} = \frac{4\pi\alpha^2 p_c}{4(q^2)^2}\frac{4M^2}{\sqrt{q^2}}\left[\frac{2}{3}\eta\left(\frac{5}{3}|G_M|^2 + \frac{48}{5}\eta^2|G_\Theta|^2\right)(1+\cos^2\Theta)\right.$$
$$\left. + \left(2|G_E|^2 + \frac{8}{9}\eta^2|G_Q|^2\right)\sin^2\Theta\right] . \qquad (A13)$$

5) $\overline{\frac{1^+}{2}} - \frac{3^-}{2}$

The constraint free amplitudes are defined by

$$\langle N^*(p^*,\lambda^*)\bar{N}(p,\lambda)|J_\mu(0)|0\rangle = e\,\bar{u}^\beta(p^*,\lambda^*)\,\Gamma_{\beta\mu}\,u(p,\lambda) , \qquad (A14)$$

$$\Gamma_{\beta\mu} = -G_1'(q_\beta\gamma_\mu - \not{q}g_{\beta\mu}) + G_2'(q_\beta p^*_\mu - p^*\!\cdot q\,g_{\beta\mu})$$
$$+ G_3'(q_\beta q_\mu - q^2 g_{\beta\mu}) , \qquad (A15)$$

and the helicity amplitudes are given by

$$\Gamma^{1/2,-1/2} = -\frac{p_c\sqrt{q^2}}{\sqrt{Q^-}}\sqrt{\frac{1}{3}}\left(-(q^2+m(M-m))\frac{2G_1'}{M} + (\sigma+q^2)G_2' + 2q^2G_3'\right) , \qquad (A16a)$$

$$\Gamma^{3/2,1/2} = \frac{p_c\sqrt{q^2}}{\sqrt{Q^-}}\left(-2M(M-m)\frac{G_1'}{M} + (\sigma+q^2)G_2' + 2q^2G_3'\right) , \qquad (A16b)$$

$$\Gamma^{1/2,1/2} = -\sqrt{q^2}\frac{p_c\sqrt{q^2}}{\sqrt{Q^-}}\sqrt{\frac{2}{3}}\left(2M\frac{G_1'}{M} - 2MG_2' - \frac{1}{M}(\sigma+q^2)G_3'\right) . \qquad (A16c)$$

6) $\overline{\frac{1^+}{2}} - \frac{3^+}{2}$

The corresponding unprimed invariants G_1, G_2 and G_3 are obtained by multiplying $\Gamma_{\beta\mu}$ in(A15) by $i\gamma_5$ from the left. The helicity amplitudes are given by the replacement $G_1' \to G_1$ and $M \leftrightarrow -M$ in Eq.(A16).

7) $\overline{\frac{1^+}{2}} - \frac{5^+}{2}$

One has

$$\langle N^*(p^*,\lambda^*)\bar{N}(p,\lambda)|J_\mu(0)|0\rangle = e\,\bar{u}^{\beta_1\beta}(p^*,\lambda^*)q_{\beta_1}\Gamma_{\beta\mu}u(p,\lambda)$$

and defines three invariants $G_1'^{(5/2)}$, $G_2'^{(5/2)}$ and $G_3'^{(5/2)}$ in analogy to (A15). The helicity amplitudes are obtained from (A16) by multiplying the r.h.s. of (A16a) and (A16c) by $\sqrt{\frac{3}{5}}\,p_c\sqrt{q^2}/M$ and (A16b) by $\sqrt{\frac{2}{5}}\,p_c\sqrt{q^2}/M$.

APPENDIX B

The relative coupling strengths of the vector mesons ρ, ω, ϕ and ψ to the $B\bar{B}$ system at $q^2 = 0$ are given by :

$\frac{1^+}{2}\frac{\overline{1^+}}{2}$

C_1^V

V	$p\bar{p}$	$n\bar{n}$	$\Sigma^+\bar{\Sigma}^+$	$\Sigma^0\bar{\Sigma}^0$	$\Sigma^-\bar{\Sigma}^-$	$\Xi^0\bar{\Xi}^0$	$\Xi^-\bar{\Xi}^-$	$\Lambda\bar{\Lambda}$	$C_0^+\overline{C_0^+}$	$C_1^{++}\overline{C_1^{++}}$
ρ	$\frac{1}{2}$	$-\frac{1}{2}$	1	0	-1	$\frac{1}{2}$	$-\frac{1}{2}$	0	0	1
ω	$\frac{1}{2}$	$\frac{1}{2}$	$\frac{1}{3}$	$\frac{1}{3}$	$\frac{1}{3}$	$\frac{1}{6}$	$\frac{1}{6}$	$\frac{1}{3}$	$\frac{1}{3}$	$\frac{1}{3}$
ϕ	0	0	$-\frac{1}{3}$	$-\frac{1}{3}$	$-\frac{1}{3}$	$-\frac{2}{3}$	$-\frac{2}{3}$	$-\frac{1}{3}$	0	0
ψ	0	0	0	0	0	0	0	0	$\frac{2}{3}$	$\frac{2}{3}$

$C_1^V + C_2^V$ in units of the magnetic moment of each particle

V	$p\bar{p}$	$n\bar{n}$	$\Sigma^+\bar{\Sigma}^+$	$\Sigma^0\bar{\Sigma}^0$	$\Sigma^-\bar{\Sigma}^-$	$\Xi^0\bar{\Xi}^0$	$\Xi^-\bar{\Xi}^-$	$\Lambda\bar{\Lambda}$	$\Lambda\bar{\Sigma}^0$	$C_0^+\overline{C_0^+}$	$C_1^{++}\overline{C_1^{++}}$
ρ	$\frac{5}{6}$	$\frac{5}{4}$	$\frac{2}{3}$	0	2	$\frac{1}{4}$	$-\frac{1}{2}$	0	1	0	1
ω	$\frac{1}{6}$	$-\frac{1}{4}$	$\frac{2}{9}$	$\frac{2}{3}$	$-\frac{2}{3}$	$\frac{1}{12}$	$\frac{1}{6}$	0	0	0	$\frac{1}{3}$
ϕ	0	0	$\frac{1}{9}$	$\frac{1}{3}$	$-\frac{1}{3}$	$\frac{2}{3}$	$\frac{4}{3}$	1	0	0	0
ψ	0	0	0	0	0	0	0	0	0	1	$-\frac{1}{3}$

$\frac{3^+}{2}\frac{\overline{3^+}}{2}$

C_1^V, C_3^V

V	$\Delta^{++}\bar{\Delta}^{++}$	$\Delta^+\bar{\Delta}^+$	$\Delta^-\bar{\Delta}^-$	$\Sigma^{*+}\bar{\Sigma}^{*-}$	$\Sigma^{*-}\bar{\Sigma}^{*-}$	$\Xi^{*-}\bar{\Xi}^{*-}$	$\Omega^-\bar{\Omega}^-$
ρ	$\frac{3}{2}$	$\frac{1}{2}$	$-\frac{3}{2}$	1	-1	$-\frac{1}{2}$	0
ω	$\frac{1}{2}$	$\frac{1}{2}$	$\frac{1}{2}$	$\frac{1}{3}$	$\frac{1}{3}$	$\frac{1}{6}$	0
ϕ	0	0	0	$-\frac{1}{3}$	$-\frac{1}{3}$	$-\frac{2}{3}$	-1

C_2^V, C_4^V are obtained by multiplying C_1^V by the proton anomalous moment $\varkappa_p = 1.79$.

$\frac{1^+}{2}\frac{\overline{3^+}}{2}$

Relative dimensionless coupling strengths C_1^V and C_2^V. For details see the main text.

V	$p\bar{\Delta}^+$	$n\bar{\Delta}^0$	$\Sigma^+\bar{\Sigma}^{*+}$	$\Sigma^0\bar{\Sigma}^{*0}$	$\Sigma^-\bar{\Sigma}^{*-}$	$\Xi^0\bar{\Xi}^{*0}$	$\Xi^-\bar{\Xi}^{*-}$	$\Lambda\bar{\Sigma}^{*0}$
ρ	1	1	$-\frac{1}{2}$	0	$-\frac{1}{2}$	$-\frac{1}{2}$	$-\frac{1}{2}$	$\sqrt{3}/2$
ω	0	0	$-\frac{1}{6}$	$\frac{1}{6}$	$\frac{1}{6}$	$-\frac{1}{6}$	$\frac{1}{6}$	0
ϕ	0	0	$-\frac{1}{3}$	$\frac{1}{3}$	$\frac{1}{3}$	$-\frac{1}{3}$	$\frac{1}{3}$	0

Figure Captions

Fig.1 Electro-magnetic form factors of the proton in the space-like region. Data from Ref.[13].

Fig.2 Electro-magnetic form factors of the neutron in the space-like region. Data from Ref.[13].

Fig.3 Cross-sections $\sigma(e^+e^- \to \frac{1}{2}^+ \frac{\overline{1}}{2}^+)$. Dashed line: $\alpha' = 0.9$, solid lines: $\alpha' = 1$; dash-dotted line: cross section according to simple dipole-law with dipole mass $m_D = 0.71$ GeV. Upper bounds Refs.[16,17].

Fig.4 Cross sections $\sigma(e^+e^- \to \frac{3}{2}^+ \frac{\overline{3}}{2}^+)$

Fig.5 $\frac{1}{2}^+ \to \frac{3}{2}^+$ transition form factors in the space-like region. Inset: Dashed lines give result of the analysis of Ref.[9]; solid lines give our fit with $c = 3$, $\alpha' = 1$ and coupling values Eq.(3). For M_{1+} our fit is not discernible from results of Ref.[9]. Main figure: Magnetic transition form factor normalized to dipole form factor ($m_D = 0.71$ GeV) (for definitions see [8]). Shaded area: Experimental band taken from Ref.[22]; solid line: our fit with the above parameter values.

Fig.6 Cross sections $\sigma(e^+e^- \to \frac{\overline{1}}{2}^+ \frac{3}{2}^+)$

Fig.7 Cross sections $\sigma(e^+e^- \to \bar{N}\, N^*)$, where $N^* = P_{11}(1470)$, $S_{11}(1535)$, $D_{13}(1520)$ and $F_{15}(1688)$.

Fig.8 Three-body cross sections $\sigma(e^+e^- \to p\bar{p}\,\pi^0, p\bar{p}\eta)$.

Fig.9 Cross sections for charmed baryon pair production.

References

1. A. C. Hirshfeld, G. Kramer and D. H. Schiller; DESY Report 74/33 (unpublished)
2. F. M. Renard; Physics Letters 47B, 361 (1973)
3. H. D. Dürr and H. Pilkuhn; Nuovo Cimento 40A, 899 (1965)
   J. Benecke and H. P. Dürr; Nuovo Cimento 56A, 269 (1968)
4. K. Fujimura, T. Kobayashi and M. Namiki; Prog. Theor. Phys. 44, 193 (1970)
   K. Fujimura, T. Kobayashi, ibid 45, 227 (1971)
5. H. Sugawara; Tokyo University of Education Report (1969), unpublished;
   I. Ohba; Progr. Theor. Phys. 42, 432 (1969);
   M. Ademollo and E. Del Guidice; Nuovo Cimento 63A, 639 (1969)
6. R. A. Brandt and G. Preparata; Phys. Rev. Lett. 21, 1530 (1970)
7. J. G. Körner, I. Bender and A. Actor; DESY Report 75/57
8. R.C.E. Devenish, T. S. Eisenschitz and J. G. Körner; DESY Report 75/48 (to be published in Phys. Rev., July 1976)
9. R.C.E. Devenish and D. H. Lyth; Nucl. Phys. B93, 109 (1975)
10. I. Bender, J. G. Körner, V. Linke and M. G. Schmidt; Nuovo Cimenta 16A, 377 (1973)
11. F. E. Close and W. N. Cottingham; Nucl. Phys. B99, 61 (1975)
12. S. Okubo; Phys. Lett. 5, (1963) 165; G. Zweig, CERN-TH 402 (1964);
    J. Iizuka, Prog. Theor. Phys. Suppl. 37 & 38 (1966) 21.
13. R. Felst; DESY Report 73/56 (unpublished)
14. M. Castellano et al.; Nuovo Cimento 14A, 1 (1973)
15. G. Höhler et al., Karlruhe Report TKP 76/1

16. M. Conversi, T. Massam, Th. Muller and A. Zichichi; Nuovo Cimento 40A, 690 (1965)

17. B. Barish et al., Proc. of the Stony Brook Conf. (1966)

18. B. Jean-Marie, private communication

19. A. Pais; Rev. Mod. Phys. 38, 215 (1966)

20. F. J. Gilman and I. Karliner; Phys. Rev. D10, 2194 (1974)

21. O. Nachtmann; Nucl. Phys. B78, 455 (1974)
J. Cleymans and F. E. Close; Nucl. Phys. B85, 429 (1975)
B. Flume-Gorczyca and S. Kitakado; Nuovo Cim. 28A, 321 (1975)

22. J. Gayler, in "Proceedings of the 8th Session of the Spring School of Experimental and Theoretical Physics, Yerevan, April 1975", (Yerevan Physics Inst., 1975).

23. W. J. Metcalf and R. L. Walker; Nucl. Phys. B76, 253 (1974)

24. J. Gayler, private communication

25. M. K. Gaillard, B. W. Lee and J. L. Rosner; Rev.Mod.Phys. 47, 277 (1975)

26. T. Muta; Lett. Nuovo Cimento 13, 661 (1975)

27. H. Kowalski and T. F.Walsh; DESY Report 76/02
S. Okuba; University of Rochester Preprint UR-559
Y. Hara; University of Tsukuba Preprint UTHEP-4 (1975)

28. G. Goldhaber et al.; SLAC-PUB-1622/LBL-4224

29. B. H. Wiik; DESY Report 75/37

30. G. S. Abrams; Stanford Conference Proceedings (Ed.W.T. Kirk), p.25 (1975)

31. G. Kramer and T. F. Walsh; Z. Physik 263, 361 (1973)

32. M. Gourdin and J. Micheli; Nuovo Cimento 40, 225 (1965).

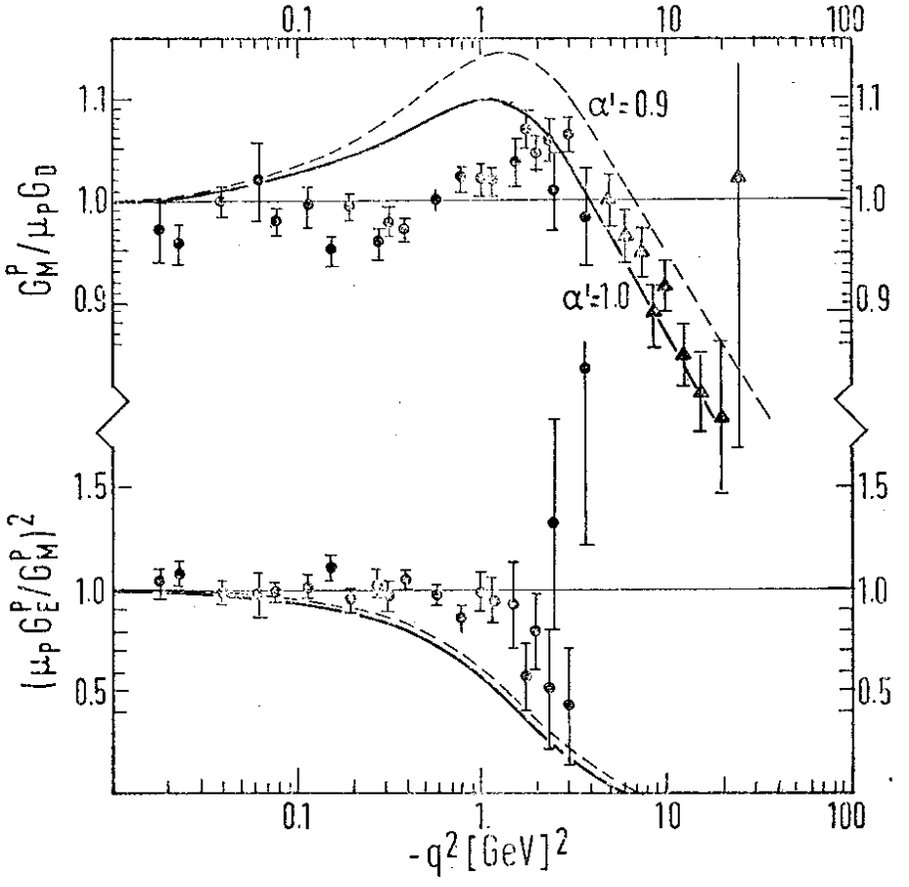

Fig.1

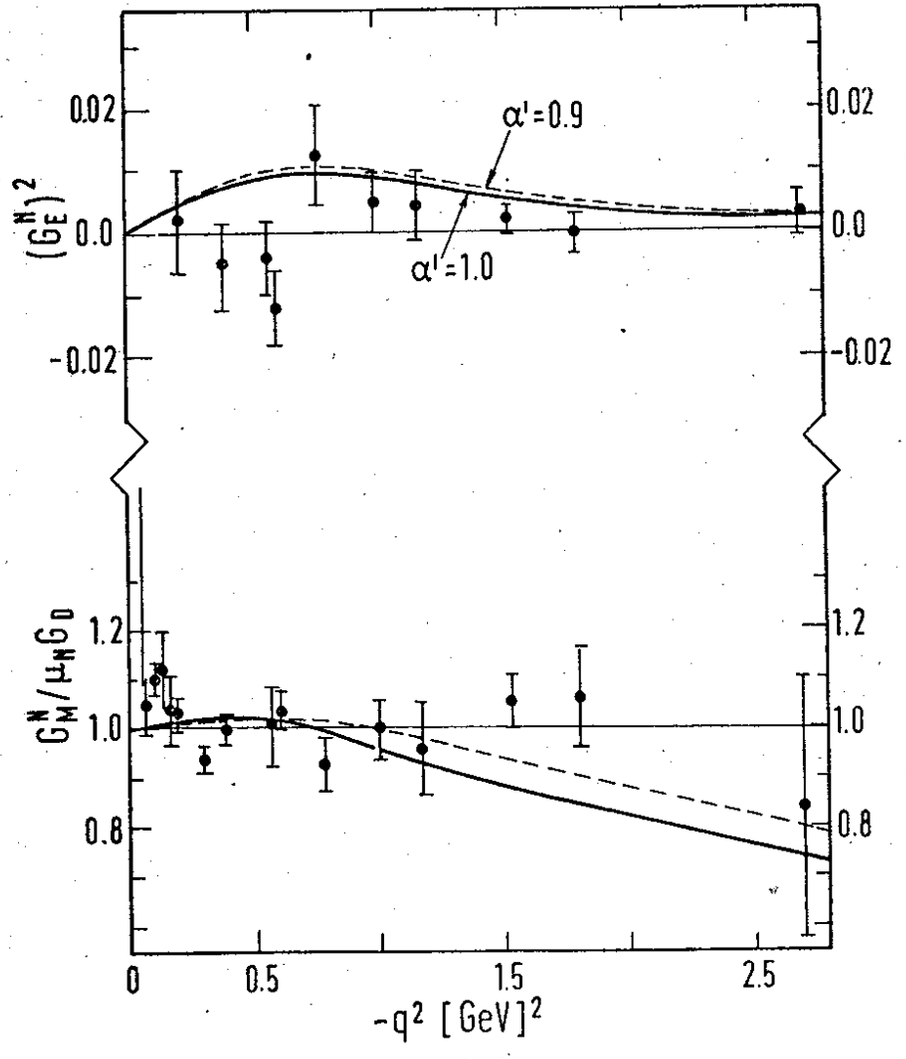
0.02
0.0
-0.02
$(G_E^N)^2$
α'=0.9
α'=1.0
1.2
1.0
0.8
$G_M^N/\mu_N G_D$
0
0.5
1.5
2.5
$-q^2$ [GeV]^2

Fig.2

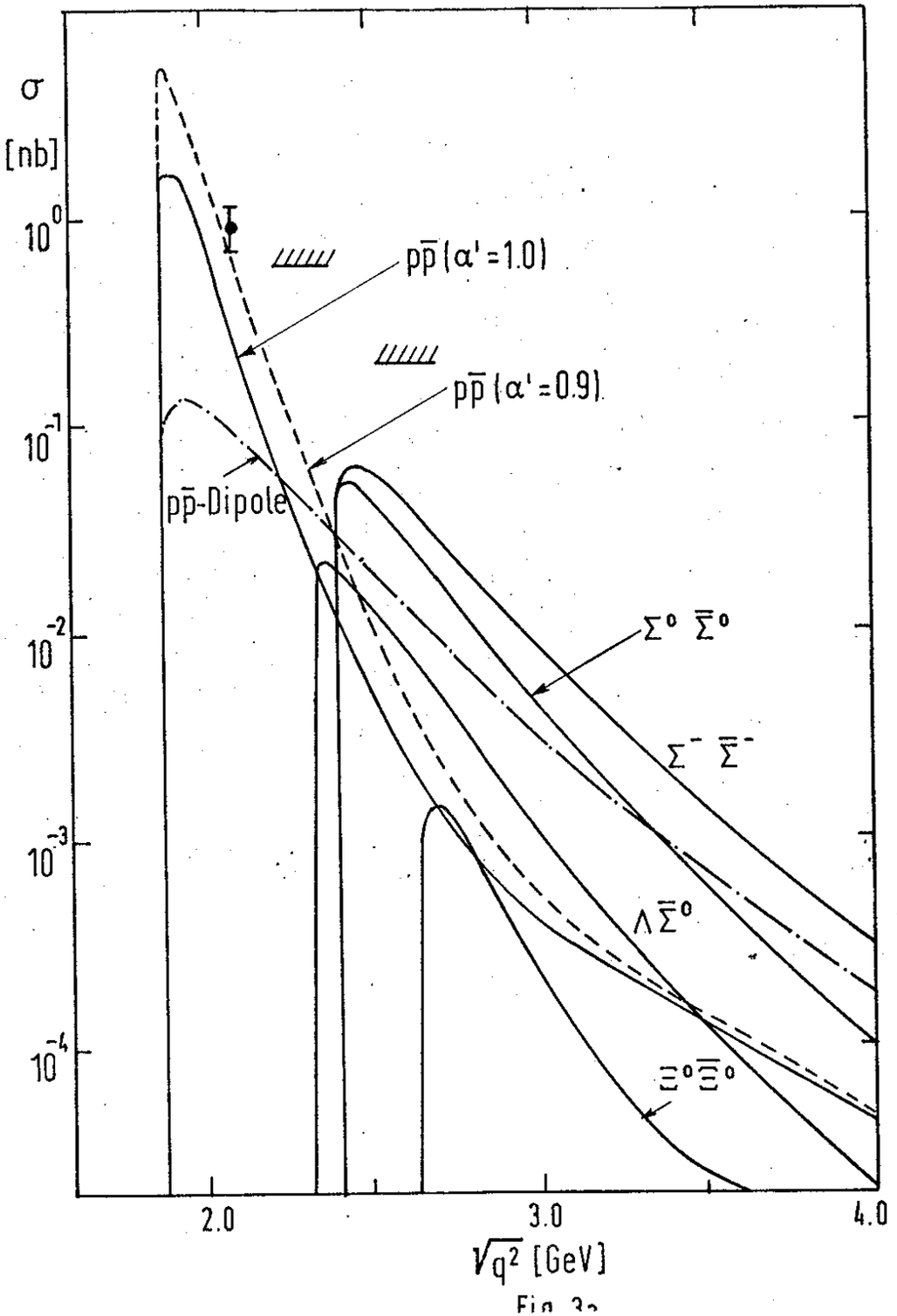
σ
[nb]
10^0
10^{-1}
10^{-2}
10^{-3}
10^{-4}
$p\bar{p}$ (α'=1.0)
$p\bar{p}$ (α'=0.9)
$p\bar{p}$-Dipole
$\Sigma^0\,\bar{\Sigma}^0$
$\Sigma^-\,\bar{\Sigma}^-$
$\Lambda\bar{\Sigma}^0$
$\Xi^0\,\bar{\Xi}^0$
2.0
3.0
4.0
$\sqrt{q^2}$ [GeV]

Fig.3a

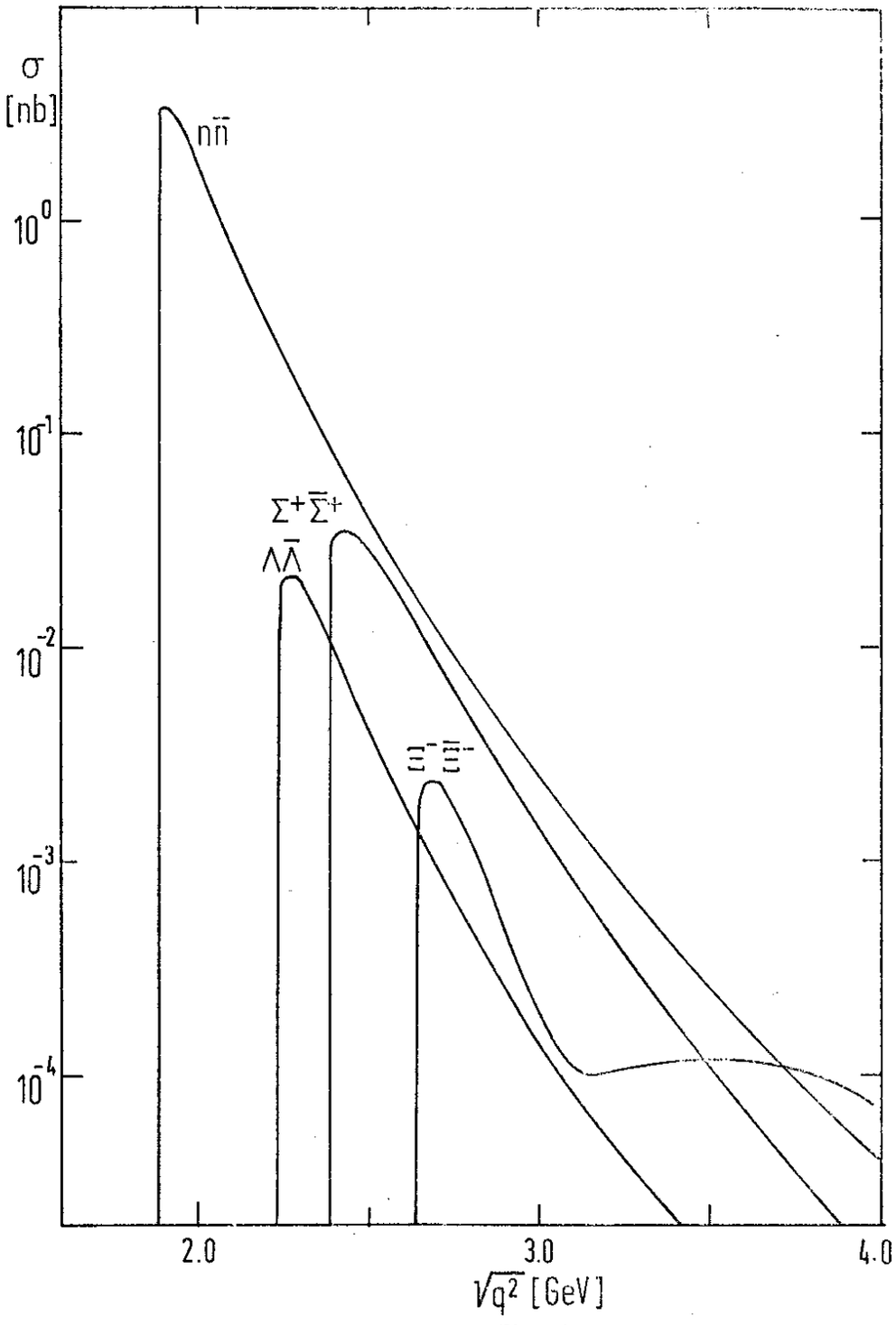
σ
[nb]
$n\bar{n}$
10^{0}
10^{-1}
10^{-2}
10^{-3}
10^{-4}
$\Sigma^{+}\bar{\Sigma}^{+}$
$\Lambda\bar{\Lambda}$
$\Xi^{-}\bar{\Xi}^{-}$
2.0
3.0
4.0
$\sqrt{q^2}$ [GeV]

Fig. 3b

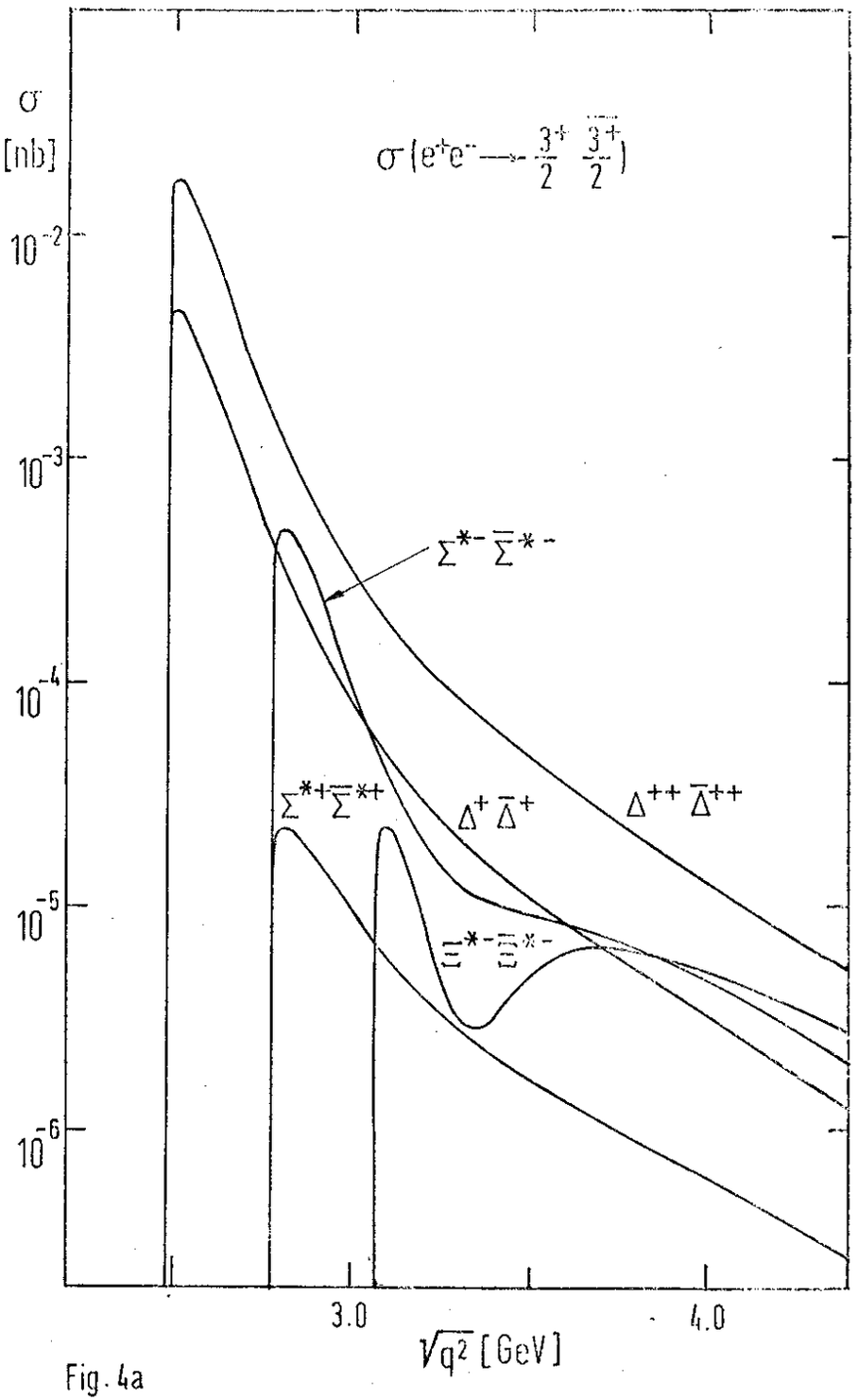
σ
[nb]
$\sigma(e^{+}e^{-} \longrightarrow \frac{3^{+}}{2}\ \frac{\bar{3}^{+}}{2})$
10^{-2}
10^{-3}
10^{-4}
10^{-5}
10^{-6}
$\Sigma^{*-}\bar{\Sigma}^{*-}$
$\Sigma^{*+}\bar{\Sigma}^{*+}$
$\Delta^{+}\bar{\Delta}^{+}$
$\Delta^{++}\bar{\Delta}^{++}$
$\Xi^{*-}\bar{\Xi}^{*-}$
3.0
4.0
$\sqrt{q^2}$ [GeV]

Fig. 4a

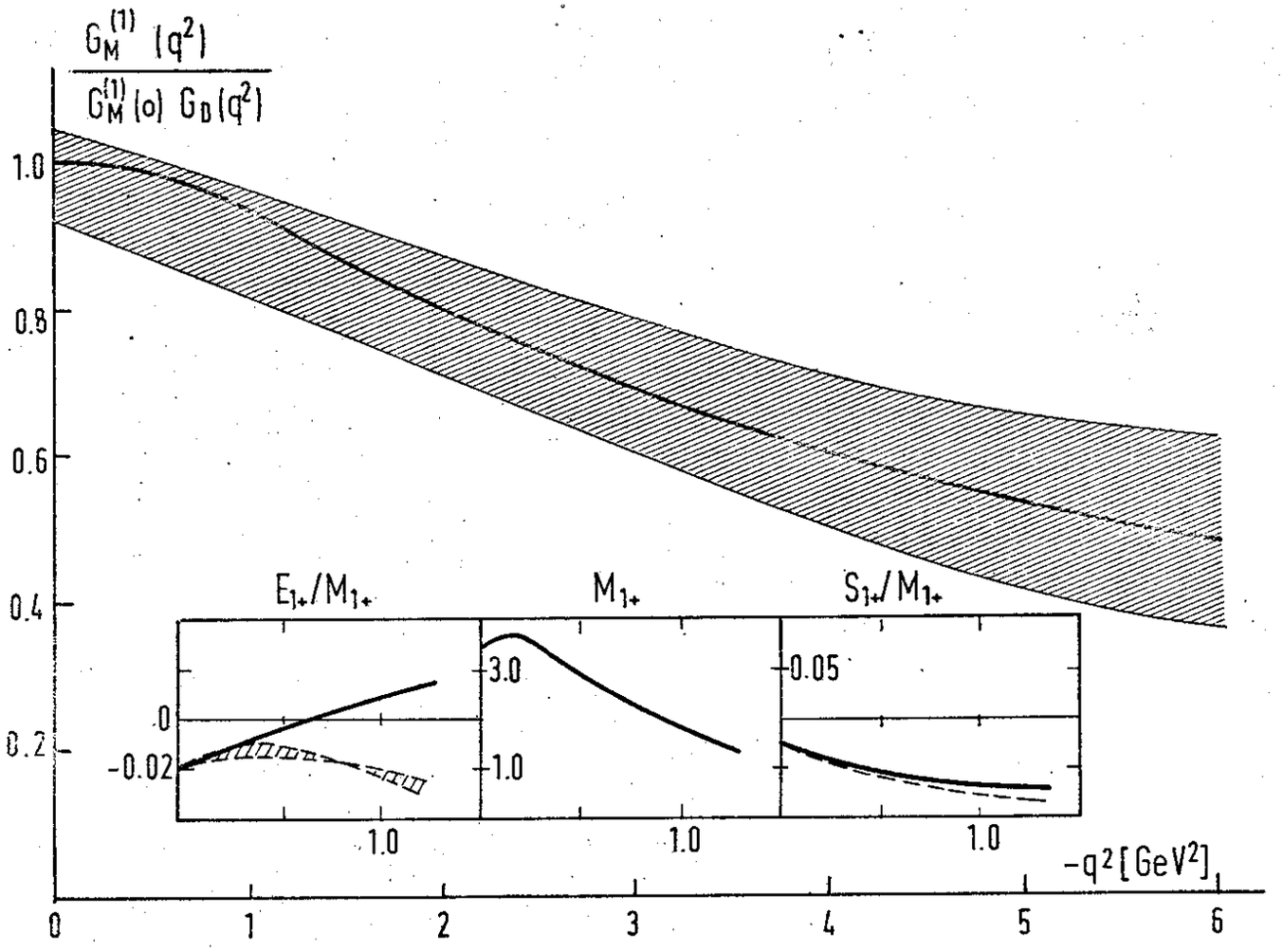
$G_M^{(1)}(q^2)$
$G_M^{(1)}(0)\, G_D(q^2)$
1.0
0.8
0.6
0.4
0.2
E_{1+}/M_{1+}
M_{1+}
S_{1+}/M_{1+}
0
-0.02
3.0
1.0
0.05
1.0
1.0
1.0
$-q^2$ [GeV^2]
0
1
2
3
4
5
6

Fig.5

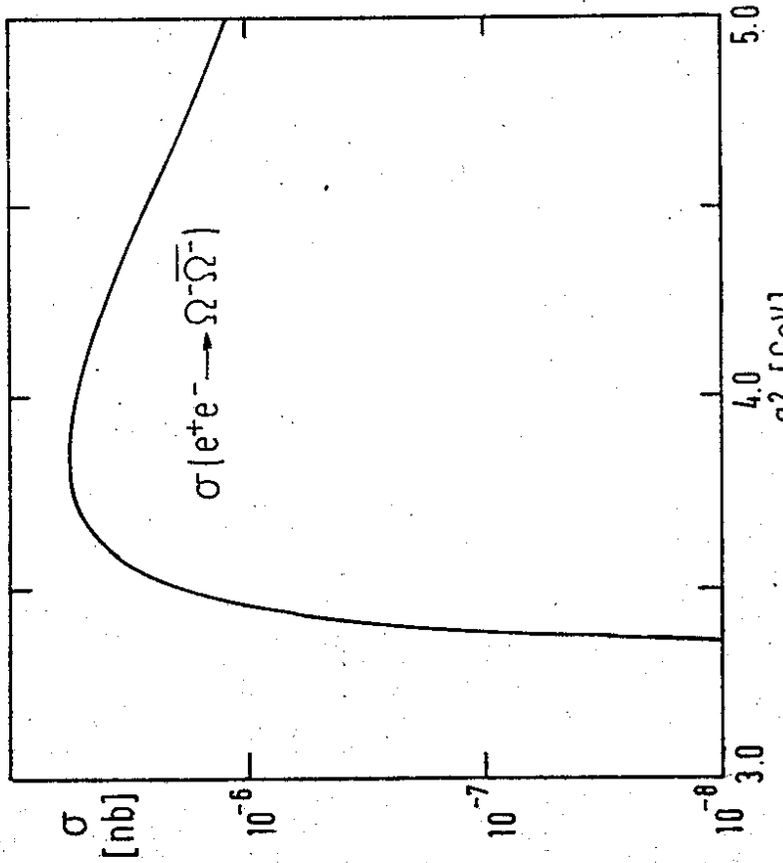
$\sigma(e^+e^- \rightarrow \Omega^-\bar{\Omega}^-)$
σ [nb]
10^{-6}
10^{-7}
10^{-8}
5.0
4.0
3.0
q^2 [GeV]

Fig.4b

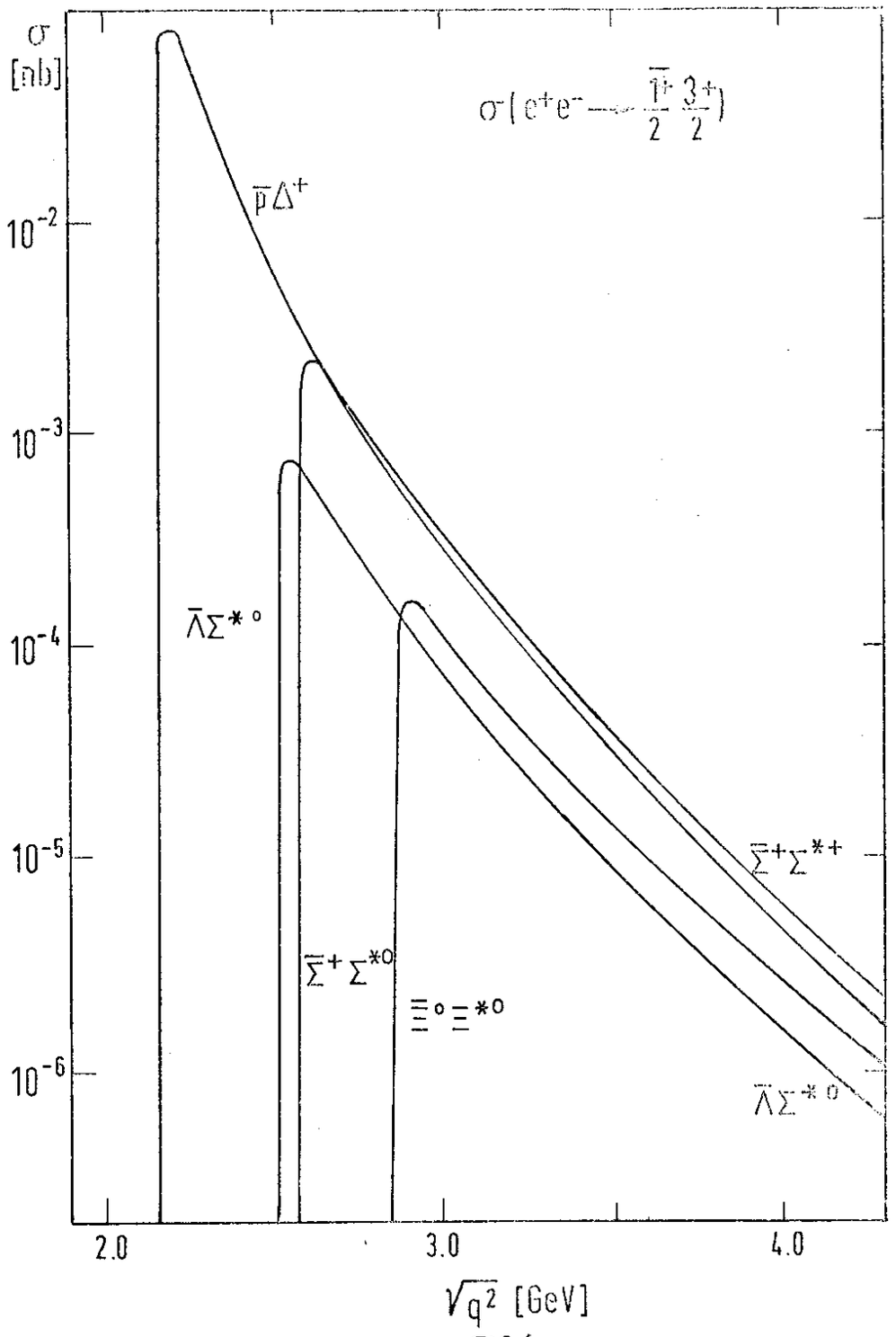
σ [nb]
$\sigma(e^+e^- \to \bar{\frac{1}{2}}^+ \frac{3}{2}^+)$
$\bar{p}\Delta^+$
$\bar{\Lambda}\Sigma^{*0}$
$\bar{\Sigma}^+\Sigma^{*0}$
$\Xi^0\Xi^{*0}$
$\bar{\Sigma}^+\Sigma^{*+}$
$\bar{\Lambda}\Sigma^{*0}$
10^{-2}
10^{-3}
10^{-4}
10^{-5}
10^{-6}
2.0
3.0
4.0
$\sqrt{q^2}$ [GeV]

Fig 6

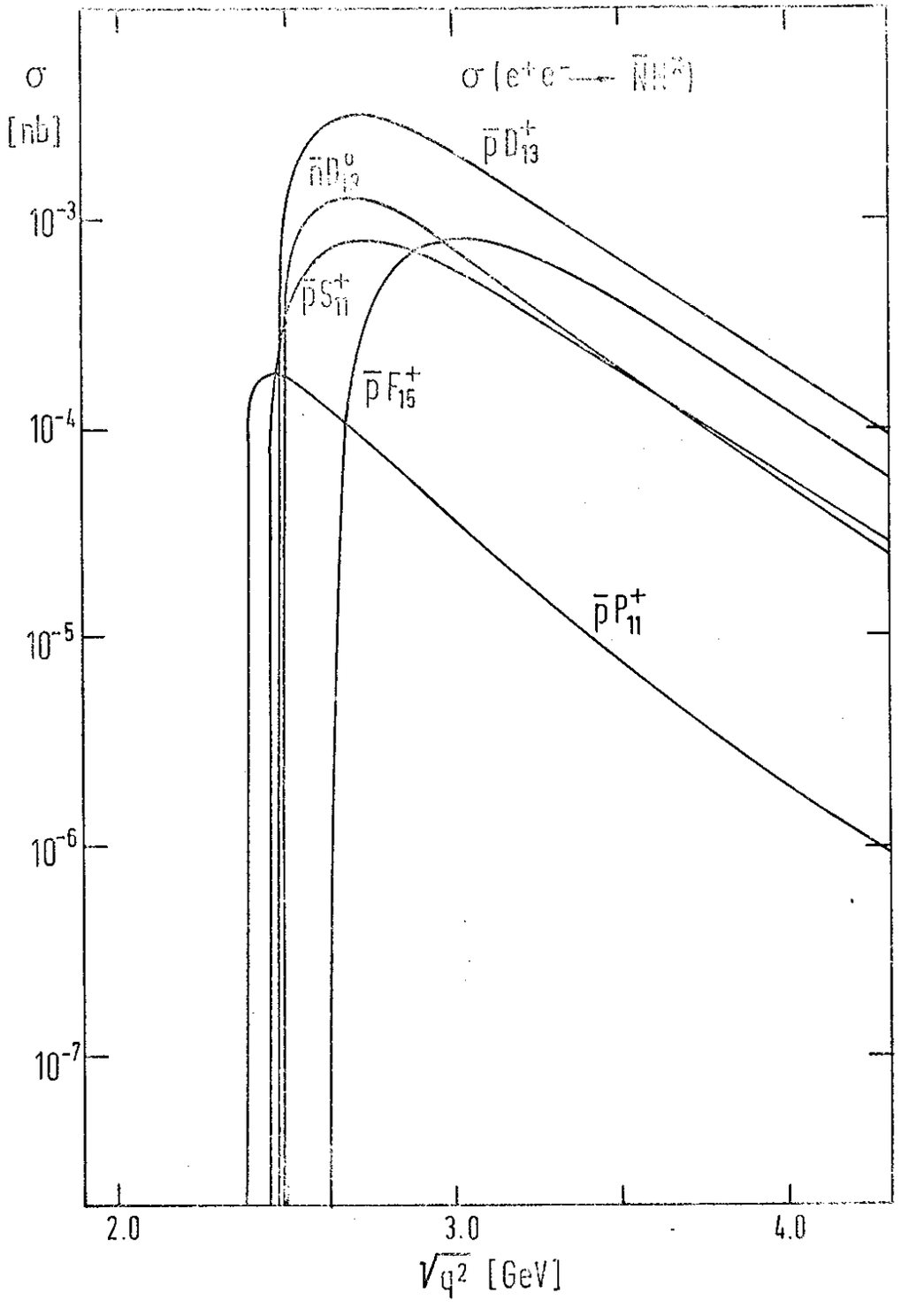
σ [nb]
$\sigma(e^+e^- \to \bar{N}N^*)$
$\bar{p}D_{13}^+$
$\bar{n}D_{13}^0$
$\bar{p}S_{11}^+$
$\bar{p}F_{15}^+$
$\bar{p}P_{11}^+$
10^{-3}
10^{-4}
10^{-5}
10^{-6}
10^{-7}
2.0
3.0
4.0
$\sqrt{q^2}$ [GeV]

Fig 7

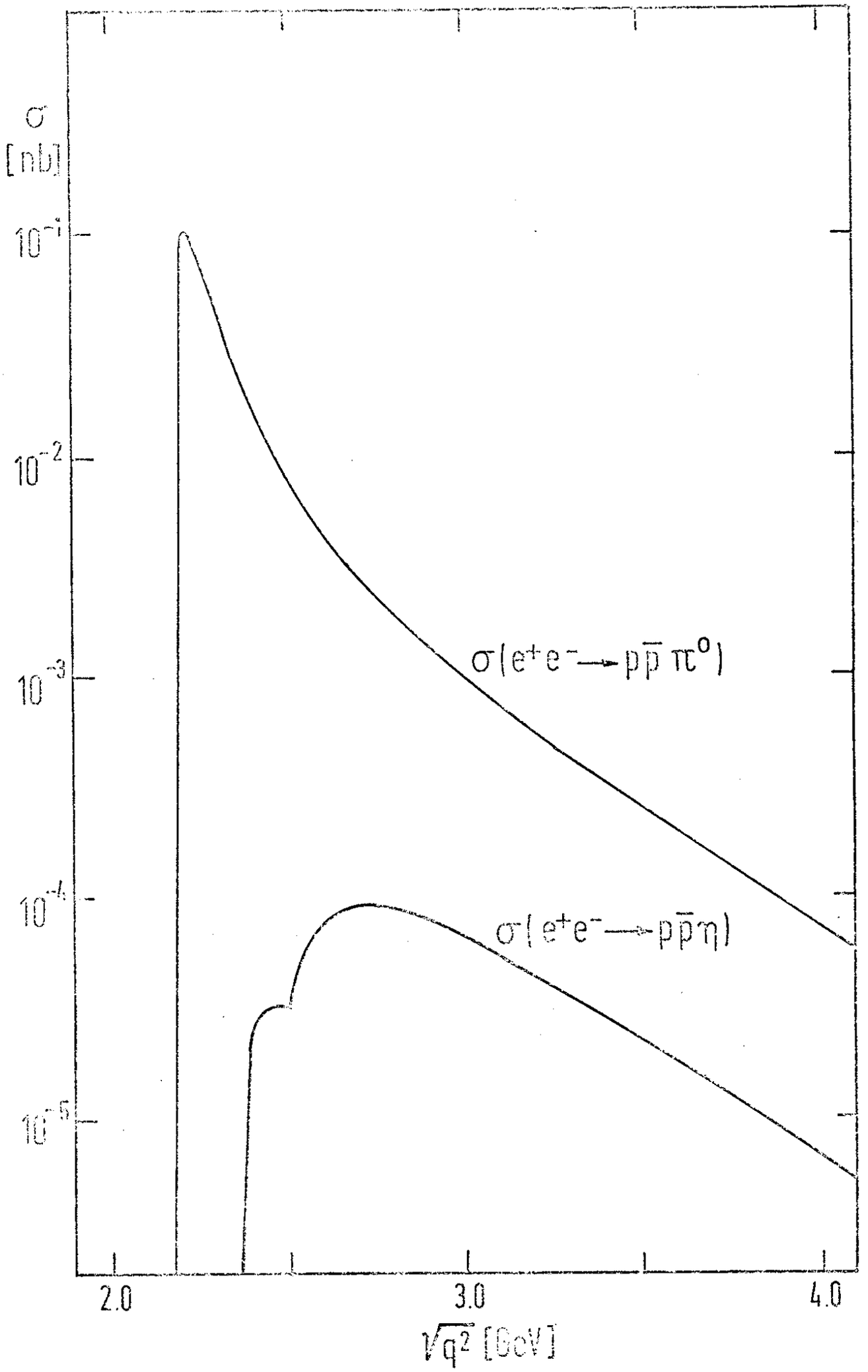

Fig. 6

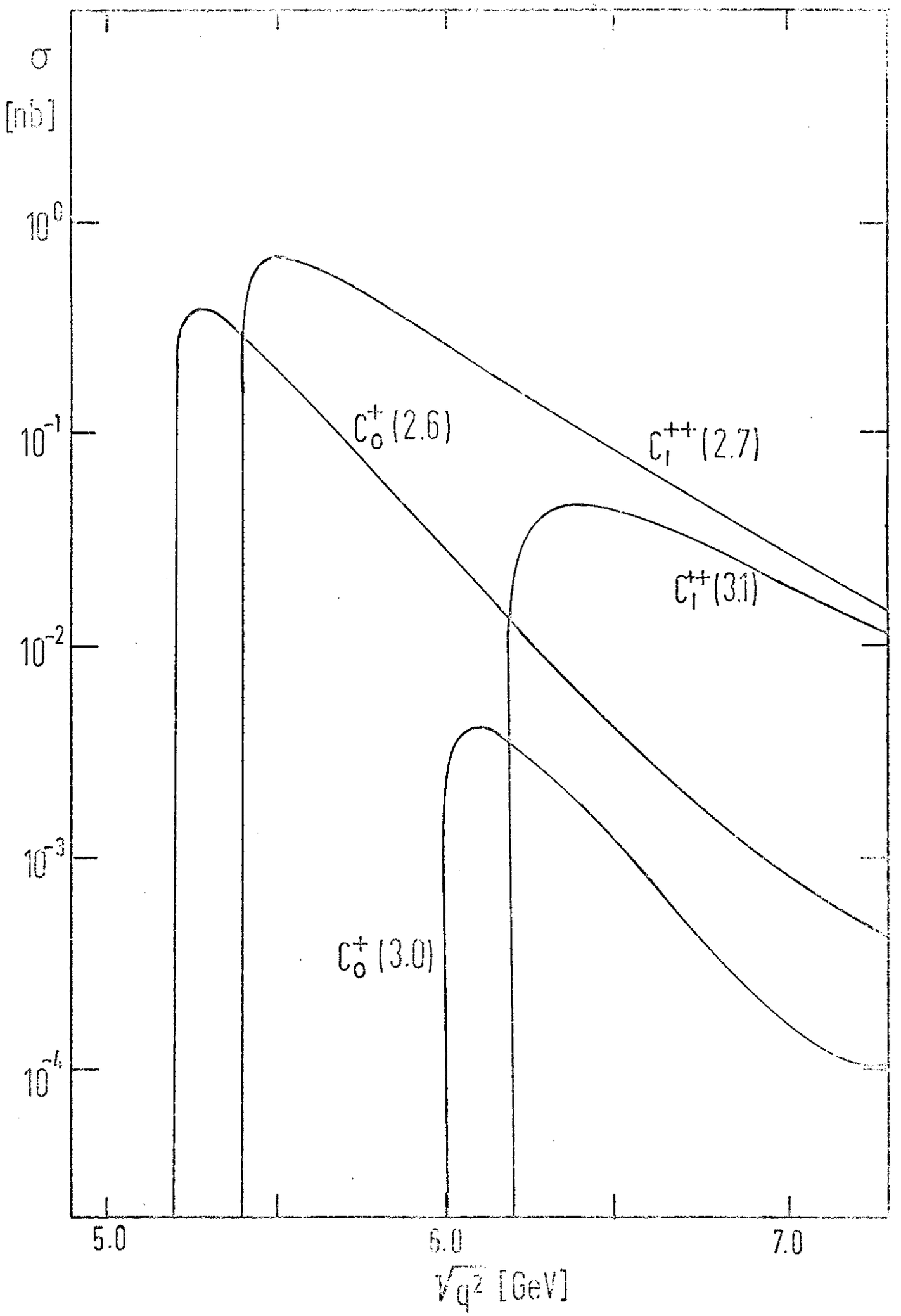

Fig. 9